JOURNAL OF SOLID STATE CHEMISTRY **107**, 452–459 (1993)

A Study of the System Li–P–Se

R. H. P. FRANCISCO

IFQSC–Universidade de São Paulo, Caixa Postal 369, 13560, São Carlos, SP, Brazil

AND T. TEPE AND H. ECKERT

Department of Chemistry, University of California at Santa Barbara, Santa Barbara, California 93106

Received September 2, 1992; in revised form April 2, 1993; accepted April 8, 1993

Compound formation in the system Li–P–Se is investigated by differential thermal analysis, differential scanning calorimetry (DSC), X-ray powder diffraction, ^{7}Li, ^{77}Se, and ^{31}P magic-angle spinning NMR, and high-temperature ^{31}P static NMR. No glasses can be formed by melt-quenching techniques. The two new crystalline phases found possess stoichiometries $Li_4P_2Se_6$ and Li_7PSe_6 and are not isostructural with their known sulfide analogs. $Li_4P_2Se_6$ crystallizes in the orthorhombic system, $a = 11.239(5)$ Å, $b = 11.811(5)$ Å, $c = 13.528(5)$ Å, $V = 1796$ Å^3, d(calc) $= 4.151$ g·cm^{-3} ($Z = 8$). It contains dimeric $[P_2Se_6]^{4-}$ units, the two P atoms of which are structurally inequivalent. Li_7PSe_6 is indexed in the cubic system, $a = 20.73$ Å, and has two crystallographically inequivalent $[PSe_4]^{3-}$ groups. In addition, the two types of selenium atoms, belonging to PSe_4^{3-} and Se^{2-} units, respectively, are distinguished by a large chemical shift difference. The thermal behavior of Li_7PSe_6 is investigated by multiple DSC studies and *in situ* high-temperature NMR, suggesting that this phase is metastable at room temperature. © 1993 Academic Press, Inc.

Introduction

Nonoxide chalcogenides which are based on sulfides, selenides, and tellurides of the III–V main group elements have recently attracted much interest as solid state materials for possible applications as low-frequency waveguides, semiconductors, and solid electrolytes (*1*, *2*). Extensive studies have revealed that glasses based on Li_2S and main group sulfides belong to the best solid lithium ionic conductors known to date (*2*). Most recently, the study of these glasses has been extended to include systems with lithium selenide such as Li_2Se–$SiSe_2$ (*3*,*4*). Unfortunately the glass forming regions in these systems are often in limited compositional ranges and the glasses usually crystallize above the glass transition. Since the addition of lithium sulfide to a binary main-group sulfide generally increases the glass-forming tendency, and since among all of the binary main-group chalcogenide systems the phosphorus–selenium system is one of the best glass-forming systems, one would expect that glasses in the Li–P–Se system should be formed rather easily. Surprisingly, this was found not to be the case. We report here the X-ray powder diffraction, differential thermal analysis (DTA), differential scanning calorimetry (DSC), and solid state NMR characterization of a wide range of compositions in the system Li–P–Se, substantiating the absence of the glass-forming tendency in this system, and providing structural characterization for the crystalline compounds.

Experimental

Powdered P (99.999%, Aldrich Chemical Co.) and Se (99.99%, Aldrich Chemical Co.)

0022-4596/93 $5.00

TABLE I

COMPOSITIONS INVESTIGATED IN THE Li-P-Se SYSTEM

Nominal composition	Observed phases
$Li_4P_2Se_6$	$Li_4P_2Se_6$
$LiPSe_2$	$Li_4P_2Se_6$ + P–Se glass
$LiPSe_3$	$Li_4P_2Se_6$ + P–Se glass
$Li_2P_2Se_5$	$Li_4P_2Se_6$ + P–Se glass
$Li_4P_2Se_7$	$Li_4P_2Se_6$ + P–Se glass
$Li_4P_2Se_5$	$Li_4P_2Se_6$ + P–Se glass
$Li_2P_4Se_{11}$	$Li_4P_2Se_6$ + P–Se glass
$Li_7P_3Se_{11}$	$Li_4P_2Se_6$ + P–Se glass
Li_7PSe_6	Li_7PSe_6[a]
Li_3PSe_4	$Li_4P_2Se_6$ + Li_7PSe_6 + P–Se glass
$Li_6P_2Se_7$	$Li_4P_2Se_6$ + Li_7PSe_6 + P–Se glass

[a] Small impurities of Li_2Se and $Li_4P_2Se_6$ are present.

were mixed in stoichiometric proportions, sealed into evacuated silica glass ampoules (10^{-3} Torr), and heated overnight at 800°C, to obtain glasses with compositions P_2Se_5, P_2Se_4, and P_2Se_3. The ampoules were furnace quenched, the resulting glasses were crushed in an argon atmosphere, mixed with Li_2Se (CERAC), and heated again at 800–900°C (ca. 16–20 hr). The temperature was decreased at a cooling rate of 10°C/hr. All the substances were handled in a stainless-steel glove box under argon atmosphere. The compositions investigated are shown in Table I. Glass formation was attempted, unsuccessfully, by quenching the ampoules in ice water.

Cu_3PSe_4, Cu_7PSe_6, and Ag_7PSe_6 were synthesized by heating sealed ampoules of the elements in stoichiometric ratio at ca. 800°C for 10 days, followed by slow cooling to 200°C. $Ag_4P_2Se_6$ was prepared in a similar fashion at 500°C (2 days). $Cd_2P_2Se_6$ and $Sn_2P_2Se_6$ were synthesized by heating the stoichiometric mixtures of the elements in evacuated quartz ampoules for 72 hr at 750 and 700°C, respectively, and subsequently cooled slowly to room temperature. All of these materials were found to be phase-pure by X-ray powder diffraction. Their solid state ^{31}P MAS, (magic-angle spinning) NMR spectra were recorded for reference purposes.

All samples were examined by X-ray powder diffraction, using a Scintag diffractometer with a Cu $K\alpha$ source. $Li_4P_2Se_6$ and Li_7PSe_6 were also studied by DTA and DSC at variable heating rates (2–10°C/min), using a Dupont 9900 thermal analysis system. Transition temperatures are reported as onset temperatures. Multinuclear MAS-NMR studies were carried out on a General Electric GN-300 wide-bore system, equipped with a magic-angle spinning probe from Doty Scientific and an Explorer fast digitizer. Samples were spun within sapphire or zirconia spinners of 7 mm o.d. at speeds between 3 and 8 kHz. For ^7Li, a spectral frequency of 116.79 MHz, a 90° pulse length of 6 μs, and a relaxation delay of 120 sec were used. ^{31}P MAS-NMR spectra were recorded at 121.65 MHz, using a 90° pulse length of 6 μs and a relaxation delay of 600 sec. ^{77}Se MAS-NMR was carried out at 57.27 MHz with a 90° pulse length of 8 μs and a 30-min relaxation delay. Chemical shifts were externally referenced to 1*M* aq. $LiNO_3$, 85% H_3PO_4, and solid CdSe, respectively. Static ^{31}P high-temperature NMR experiments on Li_7PSe_6 within sealed quartz ampoules were obtained on a modified Bruker CXP 200 spectrometer within the range from 100 to 430°C, using a probe and heater system from Doty Scientific. These spectra were recorded at 81.01 MHz, with a 6 μs pulse length and delay times ranging from 1–60 sec.

Results and Discussion

Attempts to prepare pure Li–P–Se glasses by ice-water quenching over a wide range of compositions $(Li_2Se)_x(P_2Se_3)_{1-x}$, $(Li_2Se)_x(P_2Se_4)_{1-x}$ and $(Li_2Se)_x(P_2Se_5)_{1-x}$ ($x = 0.33, 0.5$, and 0.67) were unsuccessful. To elucidate the exact stoichiometries of the crystalline phases, the Li-P-Se composition was systematically varied, and the resulting products examined by X-ray diffraction and ^{31}P solid state MAS-NMR. These experiments reveal the existence of only two crystalline phases, corresponding to the stoichiometries $Li_4P_2Se_6$ and Li_7PSe_6. All of the other compositions result in mixtures of these crystalline phases and a glassy phosphorus–selenium phase, the latter of which gives rise to a broad and unresolved ^{31}P MAS-NMR peak around 130 ppm. Table I summarizes the phase compositions of all of the samples investigated. Table II summarizes the X-ray powder patterns of the two new crystalline compounds found, $Li_4P_2Se_6$ and Li_7PSe_6. The NMR parameters of these phases are listed in Table III, and compared to those of ternary metal phosphorus selenides with analogous stoichiometries (*5–13*).

$Li_4P_2Se_6$. The stoichiometry $Li_4P_2Se_6$ is familiar from previous investigations of other metal thiophosphate and selenophosphate systems (*5–8*). Other representatives of the $M_4P_2Se_6$ stoichiometry are $Li_4P_2S_6$ (*5*), $Ag_4P_2S_6$ (two phases) (*6, 7*), and $Ag_4P_2Se_6$ (*8*), and by stoichiometric analogy, $Cd_2P_2S_6$ and $Sn_2P_2S_6$ (*13*). Our $Li_4P_2Se_6$ compound is not isostructural with any of these materials. The observed X-ray pattern for $Li_4P_2Se_6$ is shown in Table II. It was indexed in the orthorhombic system, a = 11.239(5) Å, b = 11.811(5) Å, c = 13.528(5) Å, V = 1796 Å^3, d(calc) = 4.151 g·cm^{-3} (Z = 8). The ^7Li MAS-NMR spectrum shows one resonance at 1.1 ppm (Fig. 1a). The ^{31}P MAS-NMR spectrum of $Li_4P_2Se_6$ (Fig. 2a) consists of two doublets due to P–P spin–spin coupling between two chemically inequivalent phosphorus atoms with resonances centered at 55.1 and 46.5 ppm, respectively, and a coupling constant J = 210 ± 5 Hz. This finding contrasts with the spectrum (*14*) of the homologous compound $Li_4P_2S_6$ which crystallizes in the hexagonal system (*5*) and for which these doublets are not resolved in the NMR spectrum. The spectroscopic signature present in Fig. 2a is a clear indication of a $[Se_3P–PSe_3]^{4-}$ moiety as previously characterized by MAS-NMR of various hexathiohypodiphosphates (*14, 15*). It also resembles closely that of the analogous sil-

TABLE II

OBSERVED AND CALCULATED DISTANCES, (Å), BETWEEN CRYSTALLOGRAPHIC PLANES, (*hkl*), AND RELATIVE INTENSITIES OF X-RAY DIFFRACTION LINES IN $Li_4P_2Se_6$ (a = 11.239(5), b = 11.811(5), c = 13.528(5) Å), AND IN Li_7PSe_6, (FOR A CUBIC UNIT CELL, a = 20.73 Å)

d(obs) (Å)	$h\ k\ l$	d(calc) (Å)	I(rel)
	$Li_4P_2Se_6$		
6.752	0 0 2	6.764	3
5.890	0 2 0	5.905	4
5.605	2 0 0	5.620	4
4.046	2 1 2	4.060	5
3.467	3 1 1	3.453	56
3.243	1 0 4	3.238	3
3.148	3 1 2	3.158	16
2.930	0 2 4	2.935	100
2.647	0 1 5	2.637	28
2.362	0 5 0	2.362	7
2.102	5 2 0	2.101	22
1.879	2 4 5	1.880	21
1.863	1 6 2	1.864	29
1.731	6 0 3	1.730	5
1.688	3 6 2	1.687	6
1.641	6 3 2	1.641	21
1.573	3 3 7	1.574	6
	Li_7PSe_6		
11.0	2 0 0	10.4	3
5.95	2 2 2	5.98	15
5.185	4 0 0	5.183	5
4.072	4 3 1	4.065	15
3.763	5 2 1	3.785	10
3.668	4 4 0	3.665	82
3.624	5 2 2	3.609	16
3.454	6 0 0	3.455	52
3.406	6 1 0	3.408	11
3.132	6 2 2	3.125	100
2.991	4 4 4	2.992	67
2.979	6 3 2	2.961	61
2.915	7 1 1	2.903	15
2.117	8 4 4	2.116	34
2.097	8 5 3	2.094	28
2.068	8 6 0	2.073	7
2.005	9 5 1	2.004	35
1.992	10 2 2	1.995	18
1.988	8 6 3	1.986	22
1.976	10 3 1	1.977	9
1.873	11 1 0	1.877	17
1.832	8 8 0	1.832	34
1.821	11 3 0	1.818	7
1.813	9 7 1	1.811	10
1.804	8 8 2	1.804	36
1.760	9 7 3	1.758	9
1.646	10 7 3	1.649	7
1.636	12 4 0	1.639	10
1.571	13 2 1	1.572	11

TABLE III

^{31}P CHEMICAL SHIFTS OF METAL SELENOPHOSPHATES (±0.5 ppm vs 85% H_3PO_4)

Compound	δ[ppm]	Reference
$Li_4P_2Se_6$	55.1, 46.5	This work
$Ag_4P_2Se_6$	77.5, 91.0	This work
$Cd_2P_2Se_6$	55.1	This work
$Sn_2P_2Se_6$	29.7	This work
Cu_3PSe_4	−84.5	This work
Li_7PSe_6	−80.2, −82.8	This work
Ag_7PSe_6	−51.2	[17]
Cu_7PSe_6	−30.3	This work

ver compound (Table III), for which this structure has been proven crystallographically. Note that the two doublets, which arise from ^{31}P–^{31}P spin–spin coupling, are not symmetric. As previously discussed, this effect is not an experimental artifact, but arises from the interplay of the dipole–dipole and scalar coupling between the spins and the chemical shift anisotropy (*16*). The ^{77}Se MAS-NMR spectrum (measured at 11.7 T and 5 kHz spinning speed) was not analyzed due to the presence of a number of extremely wide spinning sideband patterns with very low signal-to-noise ratios.

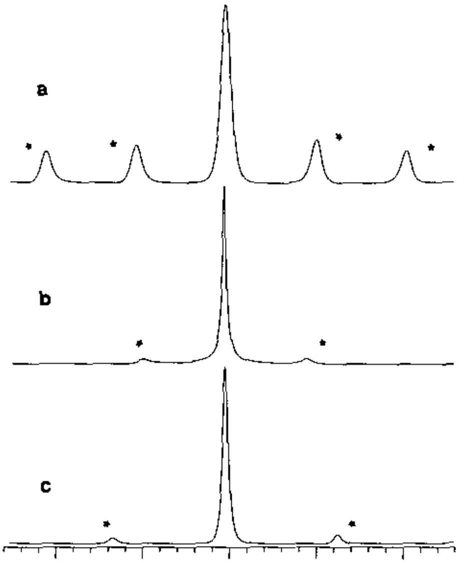

FIG. 1. Room temperature 116.7911 MHz ^{7}Li MAS-NMR spectra for (a) $Li_4P_2Se_6$, (b) Li_7PSe_6, and (c) Li_2Se. Spinning sidebands are indicated by asterisks.

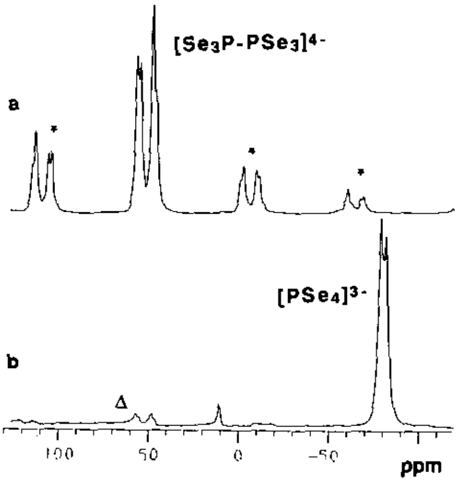

FIG. 2. Room temperature 121.65 MHz ^{31}P MAS-NMR spectra for (a) $Li_4P_2Se_6$ and (b) Li_7PSe_6. Spinning sidebands are indicated by asterisks. Δ indicates resonances from $Li_4P_2Se_6$ impurities.

DTA experiments of $Li_4P_2Se_6$ reveal two endothermic peaks at 626 and 763°C, respectively. The second, more intense one, is also observed in Li_7PSe_6.

Li_7PSe_6. Previously known representatives of the M_7PX_6 stoichiometry are Li_7PS_6 (*10*), Cu_7PSe_6 (*11, 12*), Ag_7PS_6 (*9*), and Ag_7PSe_6 (*9*). All of these phases belong to the argyrodite family (*12*). Repeated preparations with the stoichiometry Li_7PSe_6 resulted in an impure target compound, mixed with small amounts of Li_2Se and $Li_4P_2Se_6$. The X-ray powder diffraction pattern attributed to Li_7PSe_6 is shown in Table II, and has been indexed assuming a cubic cell with a = 20.73 Å. Li_7PSe_6 is not isostructural with any of the known phases with the M_7PX_6 stoichiometry.

The ^{7}Li MAS-NMR of the impure Li_7PSe_6 sample shows one resonance at 2.2 ppm (Fig. 1b). This peak presumably comprises both resonances, due to the target compound and the Li_2Se impurities, respectively. Pure Li_2Se resonates at 1.8 ppm (Fig. 1c).

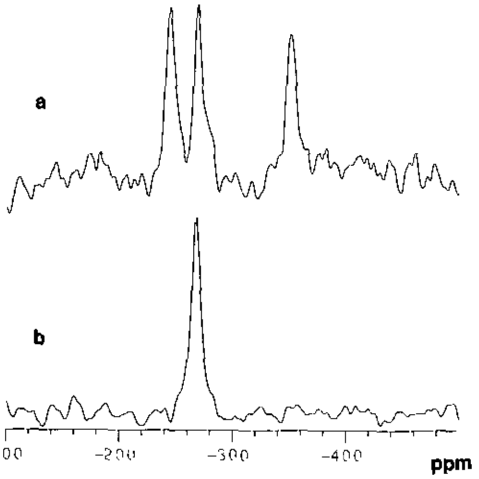

FIG. 3. Room temperature 57.27 MHz ^{77}Se MAS-NMR spectra for (a) Li_7PSe_6 and (b) Li_2Se.

The ^{31}P MAS-NMR spectrum of Li_7PSe_6 (Fig. 2b) shows two resonances, at −80.2 and −82.8 ppm. These chemical shifts are consistent with those of $[PSe_4]^{3-}$ units in other metal selenophosphates (see Table III). Contrary to the other compounds, however, the ^{31}P MAS-NMR spectrum of Li_7PSe_6 reveals the presence of two crystallographically inequivalent phosphorus atoms. This result also signifies that Li_7PSe_6 is not isostructural with any of the other argyrodites previously studied.

The ^{77}Se MAS-NMR spectrum shows three sharp resonances at −244 ppm, −268 ppm (from residual Li_2Se in the sample), and −351 ppm (Fig. 3b). In addition, an extremely wide sideband pattern is observed (not shown), with a very low signal-to-noise ratio, over the range 500 to 1500 ppm. Based on the structure of other argyrodites, we expect two fundamentally different types of selenium sites in Li_7PSe_6: those associated with the PSe_4^{3-} groups and those associated with isolated Se^{2-} species having only Li^+ ions in the first coordination sphere. In accord with past ^{77}Se MAS-NMR studies of Ag_7PSe_6 (*17*), we attribute the wide sideband pattern to the P-bonded Se atoms within the PSe_4^{3-} units. The resonances at −244 and −351 ppm are assigned to crystallographically inequivalent Se^{2-} species within the structure of Li_7PSe_6. Both resonances show essentially no spinning sideband intensity at spinning speeds above 3 kHz, revealing that the chemical shift anisotropy is very small.

Studies utilizing DTA (100 to 1000°C) and DSC (100 to 500°C) reveal the presence of four endothermic events, at 216 ± 5°C, 321 ± 10°C, 415 ± 5°C, and (not shown) 763 ± 20°C. Figure 4a shows DSC results up to 450°C. Figure 4b shows three sequential runs. The endothermic peak at 216°C does not yield a corresponding exotherm on cooling and remains absent upon reheating. We attribute this peak, which is also found in the Li_2Se starting material, to the melting of crystalline Se impurities (lit. mp. 217°C), present both in the Li_2Se used and in the Li_7PSe_6 phase produced.

The endothermic peak at 321°C shows a corresponding exotherm on cooling, indicating a reversible transition, whereas the transition at 415°C appears to be irreversible. Samples that have been cycled through this latter transition show a new exotherm at 156 ± 5°C on cooling and a corresponding new endotherm near this temperature upon reheating. In addition, such cycling gradually diminishes the intensity of the 321°C transition, further establishing the irreversibility of the transformation at 415°C (see Fig. 4b). By contrast, the new event at 156°C is absent in samples heated only to 330°C (and thus cycled through the 321°C transition only).

Finally, the DTA peak at 763°C coincides with the one observed in the $Li_4P_2Se_6$ sample. On this basis, we conclude that the peak at 415°C for Li_7PSe_6 and the one at 626°C for $Li_4P_2Se_6$ correspond to irreversible decomposition reactions producing the identical phase responsible for the event at 763°C.

Since the DSC and DTA investigations are unable to clarify the precise nature of these transformations, further insight was sought from *in situ* ^{31}P high-temperature NMR studies. Representative spectra are

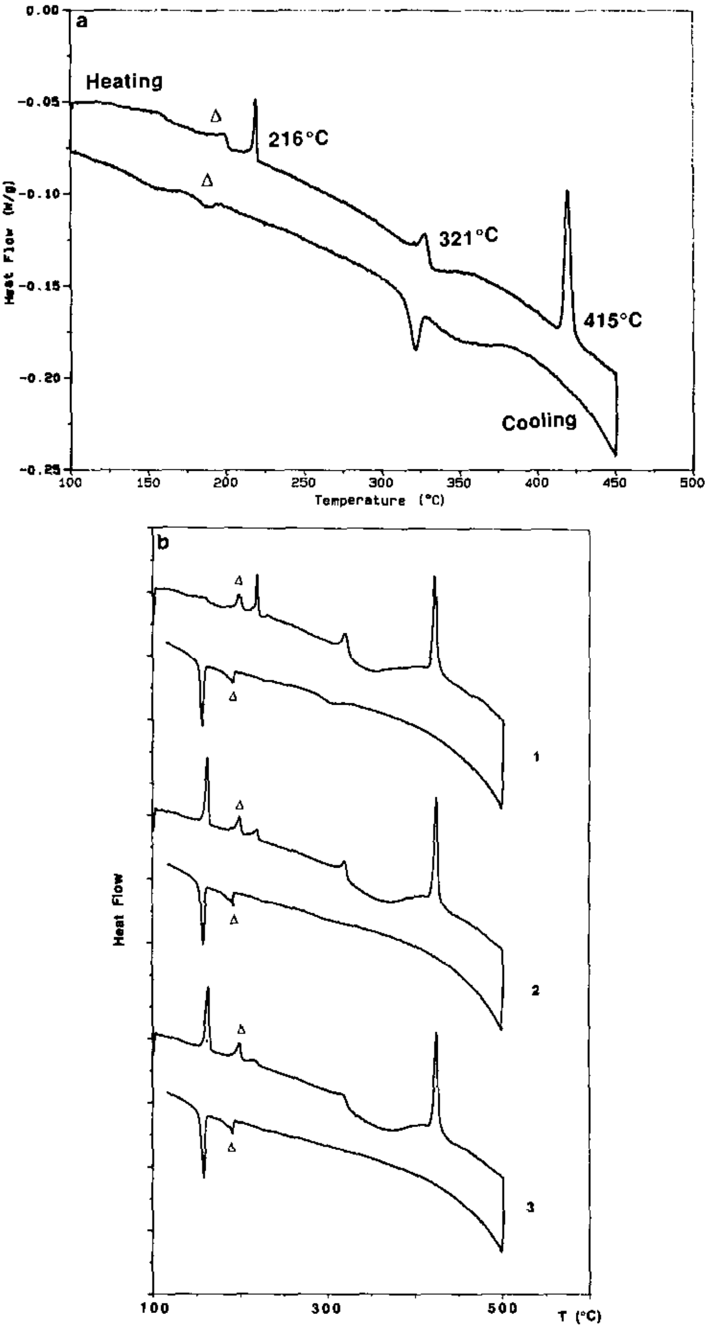

FIG. 4. (a) Differential scanning calorimetry plot of Li_7PSe_6. Positive peaks depict endotherms, negative peaks depict exotherms. An artifact resulting from an impurity in the DSC cell is marked by the symbol Δ. Heating rate was 2°C/min. (b) Differential scanning calorimetry cycling of Li_7PSe_6, showing three successive heating and cooling curves. An artifact resulting from an impurity in the DSC cell is marked by the symbol Δ. Heating rate was 5°C/min.

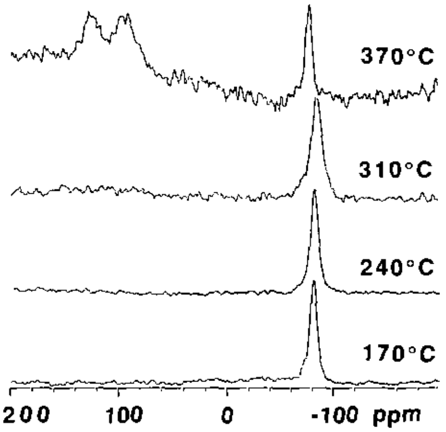

FIG. 5. Representative 81.01 MHz high-temperature ^{31}P NMR spectra of Li_7PSe_6.

shown in Fig. 5. Because these studies were carried out on static samples, the two resonances in Li_7PSe_6 are not resolved, and both $[PSe_4]^{3-}$ groups contribute to a broadened resonance around -80 ppm. There is no evident change in the ^{31}P spectra around 216°C, consistent with the interpretation of the DSC data. The spectra change significantly above 315°C, where the resonance attributed to the PSe_4^{3-} group is shifted downfield by ca. 5–6 ppm, and two new broad resonances appear around 90 and 120 ppm, a chemical shift region typical for three-coordinated phosphorus atoms (*18*). These results suggest that the 321°C transition is associated with a decomposition reaction resulting in formation of three-coordinated P atoms. As the temperature increases further, these new resonances gain in intensity; however, no further marked change is observable. Room-temperature NMR spectra of samples heated at around 430°C show that the PSe_4^{3-} group is found again at its original position; however, they also show that the three-coordinated P atoms are still present. Taken together all these experiments confirm that the endotherms at 321 and 415°C are phase-decomposition reactions, the first reversible, the second irreversible. The new thermal event at 156°C observed in the heated samples is likely due to the new phase formed above 321°C, and made permanent by the event at 415°C, containing the three-coordinate P atoms. Furthermore, the X-ray powder pattern of this sample shows a substantial increase in the intensity of the diffraction peaks due to Li_2Se.The decomposition of Li_7PSe_6 seems to be inhibited by pronounced thermal hysteresis phenomena.

Conclusions

A detailed study of the Li–P–Se system is reported, using combined X-ray diffraction, differential scanning calorimetry, and multinuclear solid state NMR. The phase field is dominated by two ternary crystalline compounds with stoichiometries $Li_4P_2Se_6$ and Li_7PSe_6 which coexist with P–Se glasses of variable stoichiometry. The thermal behavior of Li_7PSe_6 was studied in detail, indicating reversible decomposition at 321°C into Li_2Se and another phase containing three-coordinate P atoms. An additional transformation at 415°C results in irreversible decomposition, making this change permanent.

It is interesting to note that compound formation in both the systems Ag–P–Se and Li–P–Se is limited to the two stoichiometries $M_4P_2Se_6$ and M_7PSe_6, respectively, and that neither one of these two systems shows any glass-forming tendency. By contrast, the phase diagrams of the analogous phosphate and thiophosphate systems, both of which show high glass-forming tendencies, are more complex and also show much more structural variability. The structural and compositional simplicity encountered in the selenium-based systems studied here may well explain their low glass-forming tendencies.

Acknowledgments

We thank Robert Maxwell and Carri Lyda for assistance with the high-temperature NMR experiments, and Chris Hudalla for help with the ^{77}Se NMR studies. Support by the National Science Foundation, Grant DMR 89-13738 (to H. E.), is gratefully acknowledged.

Thanks are also due to the Shell Development Company (Houston) for donating a Bruker CXP-200 NMR spectrometer. R. H. P. F. is grateful for a CAPES sponsorship.

References

1. P. C. Taylor, *Mater. Res. Soc. Bull.* 36 (1987).
2. J. H. Kennedy, Z. Zhang, and H. Eckert, *J. Non-cryst. Solids* **123,** 328 (1990).
3. V. Michel-Lledos, A. Pradel, and M. Ribes, *Eur. J. Solid State Chem.* **29,** 301 (1992).
4. A. Pradel, V. Michel-Lledos, M. Ribes, and H. Eckert, *Solid State Ionics*, in press (1992).
5. R. Mercier, J. P. Malugani, B. Fahys, J. Douglade, and G. Robert, *J. Solid State Chem.* **43,** 151 (1982).
6. P. Toffoli, P. Khodadad, and N. Rodier, *Acta Crystallogr. Sect. C* **39,** 1485 (1983).
7. P. Toffoli, P. Khodadad, and N. Rodier, *Acta Crystallogr. Sect. B* **33,** 1492 (1977).
8. P. Toffoli, P. Khodadad, and N. Rodier, *Acta Crystallogr. Sect. B* **34,** 1779 (1978).
9. P. Toffoli and P. Khodadad, *C. R. Seances Acad. Sci.* **286,** 349 (1978).
10. J. F. Brice, *C. R. Seances Acad. Sci. Ser. C* **283,** 581 (1976).
11. W. F. Kuhs, M. Schulte-Kellinghaus, V. Kramer, and R. Nitsche, *Z. Naturforsch. B* **32,** 1100, (1972).
12. W. F. Kuhs, R. Nitsche, and K. Scheunemann, *Mater. Res. Bull.* **14,** 241 (1979).
13. R. Brec, G. Ouvrard, A. Louisy, and J. Rouxel, *Ann. Chim. Paris* **5,** 499 (1980).
14. H. Eckert, Z. Zhang, and J. H. Kennedy, *Chem. Mater.* **2,** 273 (1990).
15. Z. Zhang, J. H. Kennedy, and H. Eckert, *J. Am. Chem. Soc.* **114,** 5775 (1992).
16. R. K. Harris, K. J. Packer, and A. M. Thayer, *J. Magn. Reson.* **62,** 284 (1985).
17. R. Maxwell, D. Lathrop, D. Franke, and H. Eckert, *Angew. Chem. Int. Ed. Engl.* **29,** 882 (1990).
18. D. Lathrop and H. Eckert, *J. Phys. Chem.* **93,** 7895 (1989).